



## Running Title: PWV CHANGES IN 5XFAD MICE

47

### 48 Abstract:

49 Alzheimer's Disease (AD) is a global health issue, affecting over 6 million in the United States,  
50 with that number expected to increase as the aging population grows. As a neurodegenerative  
51 disorder that affects memory and cognitive functions, it is well established that AD is associated  
52 with cardiovascular risk factors beyond only cerebral decline. However, the study of  
53 cerebrovascular techniques for AD is still evolving. Here, we provide reproducible methods to  
54 measure impedance-based pulse wave velocity (PWV), a marker of arterial stiffness, in the  
55 systemic vascular (aortic PWV) and in the cerebral vascular (cerebral PWV) systems. Using  
56 aortic impedance and this relatively novel technique of cerebral impedance to comprehensively  
57 describe the systemic vascular and the cerebral vascular systems, we examined the sex-  
58 dependent differences in 5x transgenic mice (5XFAD) with AD under normal and high-fat diet,  
59 and in wild-type mice under a normal diet. Additionally, we validated our method for measuring  
60 cerebrovascular impedance in a model of induced stress in 5XFAD. Together, our results show  
61 that sex and diet differences in wildtype and 5XFAD mice account for very minimal differences  
62 in cerebral impedance. Interestingly, 5XFAD, and not wildtype, male mice on a chow diet show  
63 higher cerebral impedance, suggesting pathological differences. Opposingly, when we subjected  
64 5XFAD mice to stress, we found that females showed elevated cerebral impedance. Using this  
65 validated method of measuring impedance-based aortic and cerebral PWV, future research may  
66 explore the effects of modifying factors including age, chronic diet, and acute stress, which may  
67 mediate cardiovascular risk in AD.

68

69 **New and Noteworthy:** Here, we presented a new technique which is an application of the  
70 concept of aortic impedance to determining cerebral impedance. While aortic PWV is typically  
71 utilized to study aortic stiffness, we also developed a technique of cerebral PWV to study  
72 cerebral vascular stiffness. This method may be useful in improving the rigor of studies that seek  
73 to have a dual focus on cardiovascular and cerebral function.

74

75 **Keywords:** Cerebral Blood Flow, Aortic Impedance, Cerebral Impedance, Doppler Flow System

### 76 Introduction:

77 Alzheimer's disease (AD) is a progressive neurodegenerative disorder that affects millions  
78 of people worldwide, a rate that is expected to grow with the aging population (1). AD causes  
79 deficits in quality of life and daily living marked by a decline of memory and cognitive functions  
80 (2). A hallmark feature of AD is the accumulation of aggregated amyloid beta (A $\beta$ ) protein in the  
81 brain, which ultimately leads to synaptic dysfunction, neuronal loss, and cognitive impairment (3).  
82 In addition to genetic factors, lifestyle and environmental factors such as stress and diet have been  
83 implicated in the development and progression of AD (4). Beyond dementia, AD also impacts  
84 cardiovascular function, as the amyloid beta plaques also accumulate in the heart (1). A key risk  
85 factor of AD is hypertension, and it has been hypothesized that neuroinflammatory effects link  
86 these pathologies (5). However, the full extent of the mechanisms which link AD and  
87 cardiovascular disease remains poorly understood. Here, we sought to expand the understanding  
88 of how AD alters cardiovascular and cerebral blood flow in conditions of chronic diet changes or  
89 acute stress.

## Running Title: PWV CHANGES IN 5XFAD MICE

90 AD is well understood to cause neuropsychologic decline but is also understood to affect  
91 cardiovascular dynamics. AD importantly is shown to potentially be associated with hypertension  
92 (HTN) through the formation of neuritic plaques in cerebral vasculature and potentially limiting  
93 cerebral blood flow (6). In human populations, even with correcting for risk factors such as age,  
94 HTN reduction is correlated with increased retention of cognitive ability, indicating blood pressure  
95 treatment as a potential mechanism to treat AD (1). This blood pressure linkage to AD is especially  
96 pronounced when it comes to the systolic pressure (7). However, a past review on the matter shows  
97 the issue to be far more complicated, as many previous studies are not using standardized HTN  
98 measurements and there may be age-dependent and ethnicity-dependent influences of HTN on AD  
99 development (8). Together, this underscores the need to better understand hemodynamics in AD.

100 Hemodynamics that includes pulse wave velocity (PWV) is important to study  
101 aortic/arterial stiffness and cardiovascular function (9). Even when adjusting for factors including  
102 age, race, and disease states, National Health and Nutrition Examination Survey studies indicate PWV  
103 remains a strong predictor of overall mortality in human populations (10). Past studies looking at  
104 echocardiographic parameters in humans with AD showed that diastolic function was more heavily  
105 impacted in AD pathology, marked by increased arterial stiffness, increased atrial conduction  
106 times, reduced blood flow, and altered mitral valve velocities (11). Carotid-femoral pulse wave  
107 velocity increased aortic stiffness has also been linked as an independent predictor of cognitive  
108 impairment for both dementia and AD (12). Another longitudinal study across over 1700  
109 participants found that arterial stiffness and alterations in pulse pressure are antecedents for  
110 cognitive decline (13). PWV can further be used to distinguish vascular dementia and AD, with  
111 the former often expressing increased vascular stiffness relative to AD (14). Past studies have also  
112 highlighted the importance of looking at both PWV as well as cerebral blood flow, through MRI,  
113 with hypertensive symptoms altering heart and brain structure (15). Yet there remains controversy,  
114 as some studies have found no correlation between carotid-femoral PWV and AD (16).

115 Our primary way to study AD cardiovascular-related parameters is through 5x transgenic  
116 (5xFAD) mice, which have 5 AD-linked mutations. The 5xFAD mouse model expresses human  
117 amyloid precursor protein (APP) and presenilin 1 (PS1) mutations, leading to the rapid  
118 accumulation of A $\beta$  and the development of AD-like pathology (17). This model also bears  
119 numerous similarities to human models including A $\beta$ -butyrylcholinesterase association and  
120 hallmarks of progressive loss of cognitive function concomitant with reduced synaptic markers  
121 (18). Due to apoptotic neuron loss, 5xFAD mice display memory deficits by 4 months of age (19).  
122 This mouse model has been widely used to study the mechanisms underlying AD and to test  
123 potential therapeutic interventions. Past studies using 3x transgenic mice models highlight that  
124 with induced hypertension, mice had faster development of AD marked by upticks in A $\beta$ , amyloid  
125 plaque load, and phosphorylated tau (20). This validates that transgenic mice models retain the  
126 relationship between cerebrovascular and cardiovascular dysfunction that has been observed in  
127 AD.

128 To advance a new way of studying cerebrovascular dynamics in both wildtype and 5XFAD  
129 mice, we developed a technique to measure cerebral pulse wave velocity. The relationship between  
130 PWV and AD pathology in 5xFAD models remains unclear, especially as it comes to cerebral  
131 pulse wave velocity (cPWV), a hemodynamic parameter that has been increasingly recognized as  
132 an important predictor of cerebrovascular disease. While aortic stiffness can serve as a predictor  
133 for strokes, it is limited in detection of minor changes which precede cerebrovascular changes such

## Running Title: PWV CHANGES IN 5XFAD MICE

134 as microbleeds (21). Similar to its aortic counterpart, cPWV measures the speed at which arterial  
135 pressure or velocity waves propagate through the cerebral arteries. Measuring cerebral impedance  
136 is a novel measure of the comprehensive characterization of cerebral blood vessels, which is highly  
137 relevant as the brain is a highly vascularized organ that requires a constant supply of oxygen and  
138 nutrients, with disruptions in blood flow being linked to cognitive impairment. In AD, this remains  
139 highly relevant as it may relate to A $\beta$  clearance (8). A recent clinical trial protocol has proposed  
140 utilizing carotid-cerebral PWV as a mechanism to better understand acute ischemic strokes (22).  
141 Here, we use pulsed Doppler ultrasound to simultaneously measure the arrival of the velocity wave  
142 at two different arterial sites, one at the aortic arch and another at ophthalmic artery in the distal  
143 internal carotid artery and measure the physical distance between the two sites to estimate cerebral  
144 PWV (cPWV). Also, using carotid flow velocity and aortic blood pressure we measured cerebral  
145 impedance and impedance-based PWV (cPWV<sub>Zc</sub>) which is crucial for improving our  
146 understanding of the pathophysiology of AD (Table 1).

147 To validate our methods, we studied sex-dependent, diet-dependent, and stress-induced  
148 differences in WT and 5XFAD mice. While it is clear that females are more likely to get AD in  
149 humans, there remains a gap in the literature in understanding sex-dependent differences in  
150 cerebral hemodynamics in 5xFAD mouse models (18). Using a combination of aortic and cerebral  
151 PWV, our findings provide important insights into the relationship between PWV and AD  
152 pathology, as well as potential novel mechanisms of protection. By understanding how these  
153 factors interact to influence arterial stiffness and cognitive function, we may be able to identify  
154 new therapeutic targets for the treatment and prevention of AD.

155

### 156 Methods Before You Begin:

157 **Animals.** All animal protocols were approved by the Institutional Animal Care and Use Committee  
158 of Baylor College of Medicine in accordance with the National Institutes of Health Guide for the  
159 Care and Use of Laboratory Animals. We used 3 groups of 5xFAD mice at 4-5 months of age. The  
160 diets of the 3 groups of mice consisted of standard commercial chow (2920X Harlan Teklad,  
161 Indianapolis, IN, USA), high-fat diet (60% kCal from fat), and Equi diet () with free access to food  
162 and water (**Figure S1**). Separately, we also used 8-9 month C57BL6J mice with chow diet only.  
163 All the mouse groups are shown below.

164	<b>Animals</b>	<b>Strain</b>	<b>Male</b>	<b>Female</b>	<b>Age</b>	<b>Diet</b>
165	Group1	5xFAD	n=10	n=9	4-5mo	Normal Chow
166	Group2	5xFAD	n=10	n=9	4-5mo	HFD
167	Group3	5xFAD	n=5	n=5	4-5mo	Equi Diet (Pre & Post Stress)
168	Group4	C57BL6/J	n=5	n=5	8-9mo	Normal Chow

169 Mice were initially anesthetized with 2.5% isoflurane in the induction chamber and then  
170 transferred to a heated (37±1°C) electrocardiography (ECG) board (MouseMonitor S, Indus  
171 Instruments, Webster, TX) with the paws taped to the ECG electrodes and isoflurane maintained  
172 at 1.5% via nose cone.

## Running Title: PWV CHANGES IN 5XFAD MICE

173 **Doppler flow velocity measurements.** We used a 20 MHz Doppler probe to measure doppler aortic  
174 aortic arch velocity, ophthalmic artery velocity (representative of cerebral blood flow), and  
175 abdominal aortic velocity signals to determine cerebral PWV (cPWV) and aortic PWV (aPWV)  
176 (figure 1a). We also measured aortic outflow velocity and carotid flow velocity along with aortic  
177 blood pressure, and mitral blood flow velocity (figure 1b) to determine cardiac and cerebral  
178 hemodynamics. All signals were acquired and stored using Doppler Flow Velocity System (DFVS;  
179 Indus Instruments, Webster, TX). We measured separation distance between aortic arch and OA  
180 sites and between aortic arch and abdominal aortic sites to determine cPWV and aPWV,  
181 respectively. We measured peak and mean aortic velocities, stroke distance (Sd), aortic ejection  
182 time (ET), peak and mean aortic accelerations from aortic outflow velocity, and early peak and  
183 atrial peak velocities, E/A ratio, E deceleration time, isovolumic contraction (IVCT) & relaxation  
184 (IVRT) times from mitral inflow signals, and myocardial performance index (also known as Tei  
185 index = (IVCT + IVRT)/ET). From the carotid flow velocity signal, we calculated peak, minimum,  
186 and mean velocities, pulsatility index, and resistivity index are calculated.

187 **Blood pressure measurements.** Blood pressure measurements were made as previously described  
188 (23–25), Briefly, a 1-French (0.33mm diameter) blood pressure catheter (SPR-1,000: Millar  
189 Instruments, Inc., Houston, TX) was introduced via the isolated right carotid artery and advanced  
190 into the ascending aorta to measure aortic pressure. About 2-3 second segments of blood pressure  
191 signals were acquired (simultaneously with either aortic flow velocity or carotid flow velocity and  
192 ECG signals) with the DFVS system. Systolic (SBP), diastolic (DBP), mean (MBP), pulse  
193 pressures (PP), end-systolic pressure (ESP) and rate-pressure product (RPP) were calculated from  
194 the recorded aortic blood pressure signals.

195 **Determination of aortic and carotid impedance.** The method to determine aortic impedance was  
196 described elsewhere (22, 24-26). Aortic impedance is determined using aortic pressure-velocity  
197 relationship (figure 2a). The foot of aortic pressure waveform was aligned with the foot of the  
198 aortic velocity waveform to avoid potential errors in phase relation between pressure and velocity  
199 signals. The signals are converted to frequency domain using fast Fourier transform and impedance  
200 ( $|Z| |P|/|V|$ ) parameters (peripheral vascular resistance [ $aZ_0$ ], characteristic impedance [ $aZ_C$ ], and  
201 impedance at first harmonic [ $aZ_1$ ]) are calculated. Aortic pulse wave velocity was calculated as  
202  $aZ_C/\rho$  ( $\rho$ -density of blood). The foot of the blood pressure waveform was aligned with the foot of  
203 carotid flow velocity waveform and cerebral impedance was calculated in the same way as aortic  
204 impedance (figure 2b) and the cerebral impedance parameters (cerebral vascular resistance [ $cZ_0$ ],  
205 cerebral characteristic impedance [ $cZ_C$ ], and cerebral impedance at first harmonic [ $cZ_1$ ]) were  
206 calculated. Cerebral pulse wave velocity was calculated as  $cZ_C/\rho$  ( $\rho$ -density of blood).

207 **Calculation of parameters to determine VVC.** Elastance was determined as previously discussed  
208 (25, 26). Arterial elastance (Ea) was calculated as ESP/SV (stroke volume,  $SV = Sd * aortic$  cross-  
209  $sectional$  area), end-systolic elastance (Ees) was calculated as ESP/ESV, ventricular-vascular  
210 coupling (VVC) was calculated as Ea/Ees, and stroke work (SW) was calculated as ESP\*SV (27).

211 **Statistical analyses.** All the data are presented as mean  $\pm$  standard error of the mean (SEM). Dots  
212 represent each sample, as sample size varies throughout. Statistical analyses were performed via  
213 analysis using an unpaired T-test to compare conditions in each sex through Prism (GraphPad  
214 Software; La Jolla, USA).

## Running Title: PWV CHANGES IN 5XFAD MICE

### 218 Step-By-Step to Measure Aortic and Carotid Velocity and Blood Pressure to Determine 219 Aortic and Cerebral Impedance

220

221

#### 222 Non-invasive:

223 NOTE: Only allows for PWV measurement.

224 Before you begin: This protocol needs a Doppler system (see **Figure S2** – which shows the  
225 workflow of signals, but it does not require the pressure system for the noninvasive measurement  
226 of PWV).

- 227 1. On the day of the study, weigh the animal and anesthetize it in the induction chamber  
228 using 3.0% isoflurane (mixed with 1L/min 100% O<sub>2</sub>).
- 229 2. Transfer the animal to the heated ECG board, and place in supine position with 1.5%  
230 isoflurane supplied via a nose cone.
- 231 3. Apply artificial tears lubricant gel to the eyes to prevent dryness.
- 232 4. Apply ECG cream to the four paws and tape them to the ECG electrodes.

233 NOTE: Ensure excess gas is scavenged for the safety of the operator.

234 5. Remove the hair from a small area near sternal border and a small area near mid  
235 abdominal area.

236 NOTE: The temporal canthus site near the eye used for the internal carotid artery branch of the  
237 ophthalmic artery does not need hair removal.

- 238 6. Using a 20 MHz pulsed Doppler probe, place the tip on the chest at the aortic arch site  
239 and aim toward mid-line to find an aortic arch signal. Place the probe in a tightly held  
240 holder after the signal is found.
- 241 7. Holding the second probe by hand, place its tip at the temporal canthus of the mouse eye  
242 and aim the probe toward the internal carotid artery to measure ophthalmic artery (OA)  
243 flow velocity. Measure the separation distance between the two sites (where Doppler tips  
244 are placed).
- 245 8. Treat the Arch & OA signals as I & Q (**Figure S1**) and combine to produce signals  
246 (**Figure 1A**); save a 2-3 second segment of these signals. Determine the pulse transit time  
247 offline and calculate cPWV (see upper right-hand panel **Figure 1A**).
- 248 9. Move the second probe to the abdominal location to find the abdominal aortic signal.  
249 Measure the separation distance between the two sites.
- 250 10. Treat the Arch & Abd signals as I & Q and combine them to produce signals. Again, save  
251 a 2-3 second segment of these signals, determine pulse transit time offline, and calculate  
252 aPWV (see lower right panel in **Figure 1A**).
- 253 11. Once the measurements are made, wake the mouse up and return to the cage.

254

#### 255 Invasive:

256 Before you begin: This specific protocol needs a Doppler system (see **Figure S2**- which shows  
257 the workflow of signals), that allows for the measurement and acquisition of Doppler velocity  
258 signals and ECG and blood pressure signals, simultaneously. A Millar pressure catheter and  
259 amplifier system are needed to measure blood pressure signals. The Doppler velocity signal and  
260 blood pressure are acquired simultaneously along with ECG for the temporal alignment of  
261 signals.

262 NOTE: Avoid the usage of analgesics as this may suppress blood pressure.

## Running Title: PWV CHANGES IN 5XFAD MICE

- 263 1. On the day of the study, weigh the animal and anesthetize in the induction chamber using  
264 3.0% isoflurane (mixed with 1L/min 100% O<sub>2</sub>).
- 265 2. Transfer to heated ECG board and place in supine position with 1.5% isoflurane supplied  
266 via nose cone.
- 267 3. Apply artificial tears lubricant gel to eyes to prevent dryness.
- 268 4. Apply ECG cream to the four paws and tape them to the ECG electrodes.

269 **NOTE:** Ensure excess gas is scavenged for the safety of the operator.

- 270 5. Shave the hair from the neck area and apply hair removal cream to ensure all body hair is  
271 removed.
- 272 6. Perform a pinch test to make sure the animal is unresponsive. If responsive, adjust  
273 isoflurane level to 2.0% and then return to 1.5% and redo the pinch test.
- 274 7. Use a rectal temperature probe to monitor body temperature and adjust the heated board  
275 to maintain body temperature at 37.0±0.5 °C.

276 **NOTE:** The heated board temperature is usually higher than the body temperature, so this should  
277 be closely monitored.

- 278 8. Make a 60-70mm cut in the skin of the neck, to the right of the midline.
- 279 9. Expose the right carotid artery and cannulate with a pre-calibrated saline-soaked 1F  
280 Millar catheter and secure with a suture.

- 281 10. Advance the catheter advanced into the aorta.

282 **NOTE:** Make sure the open skin is covered with wet gauze.

283 Waveforms: (See **Figure 1B** for devices/probe placements for respective measurements)

- 284 11. Using the Millar catheter, measure aortic blood pressure signals continuously.
- 285 12. Aim a 20 MHz pulsed Doppler probe tip at right suprasternal notch, caudally towards the  
286 heart with a low angle for the measurements of aortic blood flow velocity.
- 287 13. For the measurement of carotid blood flow velocity, place the Doppler probe tip left of  
288 the midline in the neck and aim caudally towards the heart at as low an angle as possible.
- 289 14. For the measurement of mitral flow velocity, reposition the Doppler probe tip under the  
290 xiphoid and aim rostrally toward the heart.
- 291 15. Record Doppler signals. Doppler signals are processed in real time and displayed as  
292 Doppler spectrograms on the screen along with the blood pressure and ECG waveforms.
- 293 16. Record the following sets of signals/waveforms: **a.** Aortic blood pressure & flow velocity  
294 and ECG; **b.** Aortic blood pressure & carotid flow velocity and ECG; and **c.** Mitral flow  
295 velocity signals with ECG.

296 **NOTE:** For each of the signal sets, collect 2-3 second segments of data for offline analysis.

- 297 17. Extract aortic and carotid flow velocity waveforms along with respective blood pressure  
298 waveforms.
- 299 18. Calculate aortic impedance and cerebral impedance, as shown in **Figures 2A & 2B**,  
300 respectively. Using a similar method to how aortic impedance is traditionally measured,  
301 cerebral impedance is derived from pressure waveforms of carotid velocity (**Table 1**).  
302 Use aortic pressure and carotid signal to equalize these values.

303 **NOTE:** Discrete Fourier transform can be computed using a simple custom code, MATLAB, or  
304 other programs.

305

## 306 307 Representative Results

## Running Title: PWV CHANGES IN 5XFAD MICE

308 While we measured general parameters, such as body weight and aortic cross-sectional  
309 area, the aim of this study was to validate our technique across experimental conditions (**Figure**  
310 **S1**). To begin with, we looked at wildtype mice with normal chow diet at an age of 8 months old,  
311 representing a standard model. Sex-dependent differences in LV afterload were evaluated using  
312 aortic impedance, which showed non-statistically significant differences of impedance parameters  
313  $Z_p$ ,  $Z_1$ ,  $Z_c$ , or  $PWV_z$  (**Figure 3A-D**). When performing the cerebral counterpart to this  
314 measurement, while many measurements remained non-significant, females exhibited a lower  
315 cerebral  $Z_p$  (**Figure 3E-H**).

316 To recapitulate these findings in a transgenic model, we looked at sex-dependent  
317 differences in aortic and cerebral impedance in 5XFAD mice chow-fed cohort that was 5-months  
318 old. LV afterload was evaluated using aortic impedance, which showed non-statistically significant  
319 differences in impedance parameters  $Z_p$ ,  $Z_1$ ,  $Z_c$ , or  $PWV_z$  (**Figure 4A-D**), but slightly more intra-  
320 cohort variability. When examining cerebral PWV, we found that both  $Z_c$  and  $PWV_z$  were both  
321 significantly lower in female mice (**Figure 4E-H**). These findings indicate that fine differences at  
322 baseline conditions may be detected, as well as showing that the 5XFAD mice differed in sex-  
323 dependent differences, as compared to WT mice. From there, we sought to validate the  
324 applicability of this aortic and cerebral measurement method with changes in diets.

325 A cohort of 8-week-old 5XFAD mice was subject to an HFD for 12 weeks and compared  
326 to the aforementioned cohort of 5XFAD mice on a chow diet. Generally, as compared to the chow  
327 cohort, the HFD diet cohort did not exhibit a significant difference in aortic or cerebral PWV  
328 parameters (**Figure S3**). However, when looking at sex-dependent differences within the 5XFAD  
329 cohort fed an HFD, we observed that cerebral parameters no longer showed a significant  
330 difference, but aortic  $Z_c$  and  $PWV_z$  were significantly lower in female mice (**Figure 5A-H**). These  
331 results that our aortic and cerebral methods have the sensitivity to detect minute sex-dependent  
332 differences that arise as a result of changes in diet.

333 Finally, we sought to apply this method to mice undergoing an acute chronic stress  
334 condition. Prior to subjecting 5XFAD mice to stress, non-invasive parameters were collected, as  
335 described above. Looking at Tei index, a measure of myocardial performance and cerebral  
336 separation distance, another measurement allowed for by non-invasive techniques, we saw no  
337 significant differences (**Figure S4A-B**). Additionally, measuring pulse transit time (PTT), which  
338 represents the interval for the aortic or cerebral pulse pressure wave to travel from the aortic or  
339 cerebral valve to a peripheral site (27), and PWV showed no significant differences for aortic or  
340 cerebral measurements (**Figure S4C-D**).

341 Given that, this non-invasive method validated sex-dependent PWV was minimally  
342 different before stress, we subjected a cohort of 5XFAD mice to 1 hour of acute stress. When sexes  
343 were grouped together, we saw that every measurement of aortic impedance,  $Z_p$ ,  $Z_1$ ,  $Z_c$ , or  $PWV_z$ ,  
344 was significantly higher in stressed mice (**Figure 5A-D**). Additionally, cerebral  $Z_p$  and  $Z_1$  were  
345 also found to be significantly higher in the cohort subjected to stress, as compared to a non-acute-  
346 stressed chow-fed 5XFAD cohort (**Figure 5E-H**). While we investigated sex-dependent  
347 differences in the stressed cohort and between cohorts, generally these were non-significant  
348 (**Figure S5**). Together, these results validate that our method of aortic and cerebral methods can  
349 effectively use Doppler measurements to observe differential chronic diet-dependent and acute  
350 stress-induced changes in hemodynamics in 5xFAD and WT mice cohorts.

## Running Title: PWV CHANGES IN 5XFAD MICE

351

352 **Discussion:**

353 Aortic and Cerebral impedance in 5XFAD

354 When evaluating the aortic peripheral vascular resistance ( $Z_p$ ), strength of wave  
355 reflections from the periphery ( $Z_1$ ), characteristic impedance ( $Z_c$ ), and PWV we did not note a  
356 significant sex-dependent difference in both control and 5XFAD mice compared to their control  
357 counterpart (**Figure 3-4**). Notably, in both control and 5XFAD mice we did see that only females  
358 displayed increased cerebral impedance. In the case of the WT, females show a slightly lower  
359 cerebral impedance  $Z_p$ , while the 5XFAD model differentially shows decreased  $Z_c$  and PWV.  
360 This can imply that neurovascular coupling or conduction of electrical signals within the brain  
361 may be uniquely protective in females with AD. Interestingly, one past study suggested that  
362 cerebral blood flow is increased in AD risk states, suggesting a complex relationship between  
363 cPWV and AD that must be further investigated (28).

364 While 5XFAD mice serve as a strong model for human AD that has been used in the past,  
365 it lacks neurofibrillary tangles which human models would otherwise have (17). Additionally,  
366 while AD in humans has clear sex-dependent differences with increased CVD risk (33, 34), a lesser  
367 effect was observed here. This may be due to mouse estrous cycles which we did not consider here  
368 (35); thus, it is unclear whether our findings can be extrapolated to humans. Another limitation of  
369 our study is that we did not measure A $\beta$  deposition levels, which may be correlated with PWV  
370 (30), or other molecular markers of AD pathology. Therefore, it is possible that our findings do  
371 not fully capture the complex relationship between hemodynamic parameters and AD pathology.  
372 Finally, our study only examined one-time points (12 weeks), and it is possible that longer  
373 development of mice may have different effects on hemodynamic parameters and AD pathology,  
374 as the latter is linked to aging.

375 Beyond this, future studies may look at the compounding effects of other experimental  
376 changes, such as induced hypertension, as the effectors that modulate sex-dependent differences  
377 in aortic and cerebral PWV of 5XFAD mice. Furthermore, there is an unmet need of understanding  
378 how aortic and cerebral PWV changes across the aging process for 5XFAD. Aging is especially  
379 important to study in the context of 5XFAD as they present a truncated development of AD  
380 pathology compared to human counterparts, marked by lower levels of A $\beta$  with isomerized D7  
381 and logarithmic plaque deposition beginning at 2 months of age, indicating that aging can uniquely  
382 affect 5XFAD mice (29, 30). Furthermore, past studies have shown that while changes in pulse  
383 pulsatility, are more common in younger individuals, stiffness is more likely to arise in older AD  
384 patients (31, 32). While 5xFAD females had less severe cardiovascular function impairments than  
385 is observed in human AD (33, 34), it is possible that compounding factors such as age and estrous  
386 cycles are implicated in our findings (35), highlighting the importance of future studies considering  
387 stratifications across sex of PWV while considering these factors. Investigating these effectors  
388 may also pave the way for future therapies, as PWV-dependence on estrogen receptors suggests a  
389 future avenue of estrogen-driven therapies to mitigate sex-dependent differences in AD.

390

## Running Title: PWV CHANGES IN 5XFAD MICE

### 391 Aortic and Cerebral impedance in HFD

392 While a diet-dependent difference was not observed in 5XFAD, we did not that sex-  
393 dependent differences did not follow the same pattern in the chow and HFD cohorts. Notably,  
394 characteristic impedance ( $Z_c$ ; average of 2–10 harmonics of impedance modulus), and pulse wave  
395 velocity (PWV; aortic stiffness index) were both significantly lower in 5xFAD HFD females mice  
396 compared to their male counterparts (**Figure 5**). Both of these measures of aortic impedance are  
397 methods of considering the change of pressure in relation to changes in velocity to consider  
398 hydraulic external load experienced by the left ventricle (36). Reduced parameters of aortic  
399 impedance generally signify a reduced aortic wall stiffness (36). Similarly, PWV typically changes  
400 concomitantly with pulse pressure, and high PWV, a marker of arterial stiffness, is known to occur  
401 across aging and with AD (13). Even in healthy adults, PWV generally increases with aging (37),  
402 so it is possible that this sex-dependent difference may lessen in an older mice cohort. Furthermore,  
403 PWV commonly decreases alongside blood pressure in the case of medications such as anti-  
404 hypertensives (38). Notably, PWV, which is measured at end-diastolic pressure, can be  
405 independent of blood pressure, which is measured at peak systolic pressure, due to less noticeable  
406 effects of stiffness in end-diastolic (24). It is still, however, possible that the HFD-induced increase  
407 in PWV in male is simply indicative of the higher BP in the 5xFAD HFD cohort. However, given  
408 that increased PWV is commonly observed in AD (13), it may also point toward certain  
409 cardiovascular differences in the 5xFAD model.

410 Contrastingly, when looking at cerebral impedance measurements, a sex-dependent  
411 difference is no longer observed in the HFD cohort. While variability in the male cohort is high,  
412 this is unlikely to account for this difference. Thus, it is possible that at baseline, while 5XFAD  
413 females are more resistant to elevated cerebral impedance, chronic diet change ameliorates this  
414 advantage. This finding highlights the potential of understanding the confluence of sex and gender.  
415 Notably, a prior study showed that while N-acetylneurameric acid is responsible for HFD-induced  
416 increased cognitive impairment in 5xFAD, RNA-sequencing showed diet and AD have different  
417 roles in the microglia (39). This suggests that while HFD and AD may affect each other in the  
418 brain, they may remain independent effectors in the heart. Other studies have found that HFD  
419 modulates plasma metabolites more so than other factors in 5xFAD mice and amplifies the role of  
420 sex (40), showing the necessity of exploring sex-dependent differences on diet in the future. Past  
421 studies have suggested that female 5xFAD mice, while more susceptible to metabolic dysfunction,  
422 HFD may serve a protective mechanism (41).

423 One other potential avenue in which AD pathology has an interplay with HFD-induced  
424 changes are through mitochondria. Previous studies have shown that HFD had depressed  
425 respiration concomitant with reduced bioenergetics in the liver (42). In Alzheimer's Disease,  
426 mitochondria are known to decline in axons (43), in 5xFAD mice mitochondria undergo fission in  
427 an age-dependent manner which is a driving force between loss of cognitive function and  
428 pathology progression observed in 5xFAD mice (44). This loss of function may be partially  
429 attributed to oxidative stress with accumulates across aging in 5xFAD mice (45). The role of  
430 mitochondria in AD pathology is further underscored by drugs that target voltage-dependent anion  
431 channel-1 to protect against pathology by stopping mitochondria dysfunction (46). While these  
432 effects have been observed mainly to occur in neurons, future studies may explore if mitochondrial  
433 function is also affected in the heart. Notably, in HFD cases alone, mitochondrial oxidative  
434 phosphorylation is actually increased which protects against contractile function changes in heart

## Running Title: PWV CHANGES IN 5XFAD MICE

435 failure (47). This is despite increased oxidative stress, which impairs mitochondrial function,  
436 induced by HFD in the brain in mice (48). One consideration is that few studies have yet looked  
437 at oxidative stress in cardiac tissue, which may have differential regulation than neuronal oxidative  
438 stress (49). Nonetheless, these contrasting roles between HFD and 5XFAD conditions may  
439 partially explain some of the altered PWV that we observed.

440 Future studies may look at the compounding effects of other experimental changes, such  
441 as high-salt diet changes in addition to HFD, as well as measuring if there is differential plaque  
442 formation under experimental conditions of 5xFAD mice. Beyond this, the specific composition  
443 of the diet may strongly affect 5xFAD's response. For example, while in the past a HFD causes  
444 increased neuroinflammation and plaque accumulation (50), a ketogenic diet (high fat/low-  
445 carbohydrate) improved cognition through inverse effects of reducing neuroinflammation (51),  
446 which may reduce cardiovascular deficits. This may be due to the glycemic content of a diet more  
447 heavily influencing the effects on neuroinflammation (52). Thus, this suggests that depending the  
448 composition of high-fat relative to salt and carbs can alter positive or negative effects of it; thus,  
449 future studies may examine hemodynamic alterations with a high-fat, salt, and sugar diet model  
450 (53), which causes increased neuroinflammation in WT mice, to better understand the influence  
451 of diet akin to that of the western-populations on AD pathology. Beyond this, since we had middle-  
452 aged 5xFAD mice (i.e., 4-5 months), it is possible that younger or older mice would respond  
453 differently to an HFD due to altered non-linear A $\beta$  accumulation that occurs in 5xFAD mice (29).

454

### 455 Aortic and Cerebral Impedance in Acute Stress Conditions

456 Finally, we examined acute stress conditions. Despite baseline 5XFAD conditions before  
457 stress exposure, stress was significant different than the 5XFAD mice they were compared to.  
458 These results generally showed that all measurements of aortic impedance had a significant  
459 increase following stress (**Figure 6**). Additionally, cerebral impedance measures of Zp and Z1  
460 were increased. Given that chronic stress has arisen as a risk factor for AD (54)p, these findings  
461 suggest a poorly explicated interplay through which stress may contribute to AD pathology  
462 through cerebrovascular effects.

463 Notably, sex-dependent differences were not drastic in cerebral impedance of the HFD  
464 cohort (**Figure S5**). This suggests that, like an HFD challenge, while females may have slightly  
465 lower cerebral impedance at baseline in 5XFAD, these sex-dependent differences may fade under  
466 certain chronic or acute challenges. These findings suggest that the relationship between PWV and  
467 AD pathology in animal models may be more complex than previously thought and highlight the  
468 importance of studying multiple hemodynamic parameters in the context of AD. Females may be  
469 less vulnerable to AD partially due to reduced cerebral impedance Zp, however global increases  
470 in aortic and cerebral PWV following stress induction may erase sex-dependent differences.  
471 Interestingly, past studies have shown that stress in females only, and not males, leads to elevated  
472 beta-amyloid (55). This highlights that PWV and cPWV are distinct from overall beta-amyloid  
473 accumulation, and not necessarily correlative, emphasizing the importance of continuing to study  
474 PWV and cPWV in a range of conditions.

## Running Title: PWV CHANGES IN 5XFAD MICE

475        Further studies are needed to elucidate the mechanisms underlying these findings and their  
476        implications for the development and progression of AD. In conclusion, our study showed no  
477        significant changes in most of the sex-dependent hemodynamic parameters examined, with the  
478        most pertinent change but confirmed the deleterious effects of stress, which displayed slight sex-  
479        dependent differences.

### 480        Conclusions

481        5XFAD mice are important new experimental models for the study of Alzheimer's Disease  
482        (17), but such models have limited research evaluating their *in situ* global cardiovascular function.  
483        Together our data also highlight that AD pathology should not only be considered in the context  
484        of tau pathology and cognitive decline but aortic and cerebral impedance metrics as well. In  
485        example, recent studies have demonstrated that Resveratrol can reduce HFD-induced accelerated  
486        cognitive decline in 5xFAD through proteolytic mechanisms (56), but these same pathways may  
487        not change HFD-induced cardiovascular remodeling. Thus, the impact of AD on cardiovascular  
488        parameters, especially under altered environmental states must be considered. Beyond using  
489        noninvasive measurements of Doppler mitral inflow and aortic flow velocity, invasive  
490        measurements of aortic and LV pressure, and the calculated aortic impedance, we also evaluated  
491        cerebral impedance.

492        In the future, cPWV may also aid in the early detection and monitoring of other  
493        neurological disorders. While arterial PWV may serve as a mechanism to explore cerebral  
494        perfusion, cerebral microbleeds have arisen as markers that are important to study in AD (8). Other  
495        studies have also shown that glutamate chemical exchange saturation transfer has been observed  
496        to concomitantly decrease with cerebral blood flow in 5XFAD mice, suggesting other novel  
497        imaging techniques that can potentially be used alongside cPWV (57). Another promising  
498        technique is 4D flow MRI, which has been used to show increased transcranial PWV in AD (58).  
499        Therefore, further studies are needed to elucidate the mechanisms underlying how cPWV and other  
500        innovative techniques may explore AD in 5XFAD and other models.

### 501        Limitations:

502        Study: There are several limitations to this study that must be considered when interpreting the  
503        results. While 5xFAD mice have many similarities to AD pathology in humans, it lacks  
504        neurofibrillary tangles and may have altered cardiac pathways which are poorly elucidated.  
505        Different mouse models of AD also respond to HFD differently (59, 60), while it remains unclear  
506        which most closely mimics that of humans which limits the ability to extrapolate findings to AD  
507        (17, 61). Beyond this, while past studies have clearly shown HFD-induced accelerated cognitive  
508        decline in 5xFAD mice (56), we did not specifically look at this or correlate brain hemodynamics  
509        or other neuronal molecular markers of AD pathology with cardiovascular stiffness changes. While  
510        we sought more to understand the impact of 5xFAD condition on diet-induced changes, it is  
511        possible there are additional neglected links between hemodynamics in the opposite regulation of  
512        AD. While we began an HFD at 5 months of age, the age mice can affect response to HFD, with  
513        past studies showing that HFD feeding before 3 months of age can have protective effects against  
514        cognitive decline (62). Past studies also observed high- and low-weight cohort differences in  
515        response to HFD in 5xFAD, which we did not see, is exacerbated in female mice (62).

## Running Title: PWV CHANGES IN 5XFAD MICE

516 **Methods:** Generally, these models are highly reproducible and adapted from existing aortic PWV  
517 measurements, so they require minimal new equipment. However, an important limitation is that  
518 wall motion must be converted to wave form in mice.

## 519 FUNDING

520 This work is supported by National Institute of Health (NIH) NIDDK T-32, number DK007563  
521 entitled Multidisciplinary Training in Molecular Endocrinology to Z.V.; NSF MCB #2011577I  
522 to S.A.M.; The UNCF/Bristol-Myers Squibb E.E. Just Faculty Fund, Career Award at the  
523 Scientific Interface (CASI Award) from Burroughs Wellcome Fund (BWF) ID # 1021868.01,  
524 BWF Ad-hoc Award, NIH Small Research Pilot Subaward to 5R25HL106365-12 from the  
525 National Institutes of Health PRIDE Program, DK020593, Vanderbilt Diabetes and Research  
526 Training Center for DRTC Alzheimer's Disease Pilot & Feasibility Program. CZI Science  
527 Diversity Leadership grant number 2022- 253529 from the Chan Zuckerberg Initiative DAF, an  
528 advised fund of Silicon Valley Community Foundation to A.H.J.; National Institutes of Health  
529 grants R01HL147818 and R01HL144941 (A. Kirabo). Its contents are solely the responsibility of  
530 the authors and do not necessarily represent the official view of the NIH. The funders had no role  
531 in study design, data collection and analysis, decision to publish, or preparation of the  
532 manuscript.

## 533 Disclosures

534 Dr. Reddy is a collaborator and consultant with Indus Instruments, Webster, TX. All other authors  
535 have no competing interests.

## 536 Author Contributions

537 A–M - 3456, –N - 3456, –V - 3456, H–B - 34, –G - 34, –V - 34, –B - 34, –E - 34, –A - 34, AM –  
538 34, ES-34, AC-34, JD -34, DS – 34, SD – 34, T–P - 23, J–G - 678, –E - 678, –D - 678, M–E - 7,8,  
539 G–T - 5678, A–H - 5678, A–R - 12345678

540 1 Conceived and designed research, 2 Performed experiments and Data collection, 3 Data analysis,  
541 4 Prepared figures, 5 Interpretation of results, 6 Drafted manuscript, 7 Edited and revised  
542 manuscript, 8 Approved final version of manuscript.

## 543 References

544

## 545 Figure Legend:

546 **Figure 1: (A)** Experimental setup to noninvasively measure cerebral (at ophthalmic artery, OA)  
547 & aortic pulse wave velocity. One probe is fixed at the aortic arch and the other probe is switched  
548 between ophthalmic artery or abdominal aorta sites for Arch-OA combined signals or Arch-Abd  
549 combined signals. Electrocardiography (ECG) waveform is shown for timing. **(B)** Experimental  
550 setup to measure aortic blood flow velocity, aortic blood pressure and) ECG in mice. The probe is  
551 repositioned at carotid artery (shown in the right panel along with pressure & ECG signals). The  
552 probe is repositioned again to measure mitral flow velocity (waveform not shown).

## Running Title: PWV CHANGES IN 5XFAD MICE

553 **Figure 2: (A)** Procedure to calculate aortic impedance – conversion of time domain signals to  
554 frequency domain spectrums and calculation of impedance modulus ( $|Z(f)| = |P(f)|/|V(f)|$ ).  $Z_c$  is  
555 calculated as the average of  $Z_2$  to  $Z_{10}$  harmonics. **(B)** Procedure to calculate cerebral impedance –  
556 conversion of time domain signals to frequency domain spectrums and calculation of impedance  
557 modulus ( $|Z(f)| = |P(f)|/|V(f)|$ ).  $Z_c$  is calculated as the average of  $Z_2$  to  $Z_{10}$  harmonics.

558 **Figure 3:** Parameters of aortic and cerebral impedance sex-dependent differences in chow-fed 8-  
559 month-old wildtype (C57BL6J) mice. **(A)** Total peripheral resistance ( $Z_P$ ), **(B)** impedance at first  
560 harmonic ( $Z_1$ ), **(C)** characteristic impedance, ( $Z_c$ ) **(D)** and impedance-based pulse wave velocity  
561 (PWV) in aortic and **(E-H)** cerebral impedance. Data are presented as mean $\pm$ SEM (n = 5/group).  
562 \* represents p <0.05, ns indicates a statistically non-significant relationship, as determined  
563 through an unpaired t-test.

564 **Figure 4:** Parameters of aortic and cerebral impedance sex-dependent differences in chow-fed 5-  
565 month-old 5XFAD mice. **(A)** Total peripheral resistance ( $Z_P$ ), **(B)** impedance at first harmonic  
566 ( $Z_1$ ), **(C)** characteristic impedance, ( $Z_c$ ) **(D)** and impedance-based pulse wave velocity (PWV) in  
567 aortic and **(E-H)** cerebral impedance. Data are presented as mean $\pm$ SEM (n = 9-10/group). \*  
568 represents p <0.05, ns indicates a statistically non-significant relationship, as determined through  
569 an unpaired t-test.

570 **Figure 5:** Parameters of aortic and cerebral impedance sex-dependent differences in high fat  
571 diet-fed 5-month-old 5XFAD mice. **(A)** Total peripheral resistance ( $Z_P$ ), **(B)** impedance at first  
572 harmonic ( $Z_1$ ), **(C)** characteristic impedance, ( $Z_c$ ) **(D)** and impedance-based pulse wave velocity  
573 (PWV) in aortic and **(E-H)** cerebral impedance. Data are presented as mean $\pm$ SEM (n = 9-  
574 10/group). \* represents p <0.05, ns indicates a statistically non-significant relationship, as  
575 determined through an unpaired t-test.

576 **Figure 6:** Parameters of aortic and cerebral in pre-stress and stressed state of 5-month-old  
577 5XFAD mice. **(A)** Total peripheral resistance ( $Z_P$ ), **(B)** impedance at first harmonic ( $Z_1$ ), **(C)**  
578 characteristic impedance, ( $Z_c$ ) **(D)** and impedance-based pulse wave velocity (PWV) in aortic  
579 and **(E-H)** cerebral impedance. Data are presented as mean $\pm$ SEM (n = 10/group). \*, \*\*  
580 represents p <0.05, p<0.01, respectively, and ns indicates a statistically non-significant  
581 relationship, as determined through an unpaired t-test.

582

### 583 Supplementary Files:

584 **Supplementary Figure 1:** Workflow of inducing a high-fat diet or stress experimental  
585 conditions in 5XFAD mice.

586 **Supplementary Figure 2:** Flow of Doppler, electrocardiography (ECG), and blood pressure  
587 (BP) signals from the animal to the transceiver and amplifier to generate the Doppler inphase (I)  
588 and quadrature (Q) audio signals, ECG, and BP signals. The Doppler Flow Velocity System  
589 (DFVS) hardware consists of a high-speed digitizer which sends the digitized I/Q, ECG, & BP to  
590 the DFVS software for acquisition, display, storage, and analysis.

## Running Title: PWV CHANGES IN 5XFAD MICE

591 **Supplementary Figure 3:** Parameters of aortic and cerebral impedance in a mixture of male and  
592 female 5XFAD mice on chow and high-fat diets. **(A)** Total peripheral resistance ( $Z_P$ ), **(B)**  
593 impedance at first harmonic ( $Z_1$ ), **(C)** characteristic impedance, ( $Z_C$ ) **(D)** and impedance-based  
594 pulse wave velocity (PWV) in aortic and **(E-H)** cerebral impedance. Data are presented as  
595 mean $\pm$ SEM (n = 19/group). ns indicates a statistically non-significant relationship, as determined  
596 through an unpaired t-test.

597 **Supplementary Figure 4:** Parameters of aortic and cerebral impedance in 5XFAD mice  
598 measured through noninvasive methods in males and females. **(A)** Myocardial performance  
599 index (Tei index), a measure of the overall function of the heart, which takes into account  
600 systolic and diastolic function, as calculated by (IVCT+IVRT)/ET. **(B)** Cerebral separation  
601 distance. **(C)** Pulse transit time and **(D)** impedance-based pulse wave velocity (PWV) in aortic  
602 and **(E-F)** cerebral parameters. Data are presented as mean $\pm$ SEM (n = 5/group). ns indicates a  
603 statistically non-significant relationship, as determined through an unpaired t-test.

604 **Supplementary Figure 5:** Parameters of aortic and cerebral impedance sex-dependent  
605 differences in non-stressed and stressed 5XFAD mice. **(A)** Total peripheral resistance ( $Z_P$ ), **(B)**  
606 impedance at first harmonic ( $Z_1$ ), **(C)** characteristic impedance, ( $Z_C$ ) **(D)** and impedance-based  
607 pulse wave velocity (PWV) in aortic and **(E-H)** cerebral impedance. Data are presented as  
608 mean $\pm$ SEM (n = 5/group). \* represents p <0.05, ns indicates a statistically non-significant  
609 relationship, as determined through an unpaired t-test.

610

611 **Supplementary Table 1:** Summary of Pulse Wave and Cerebral Impedance Measurements  
612 Utilized.

613

614

615

616

617

618

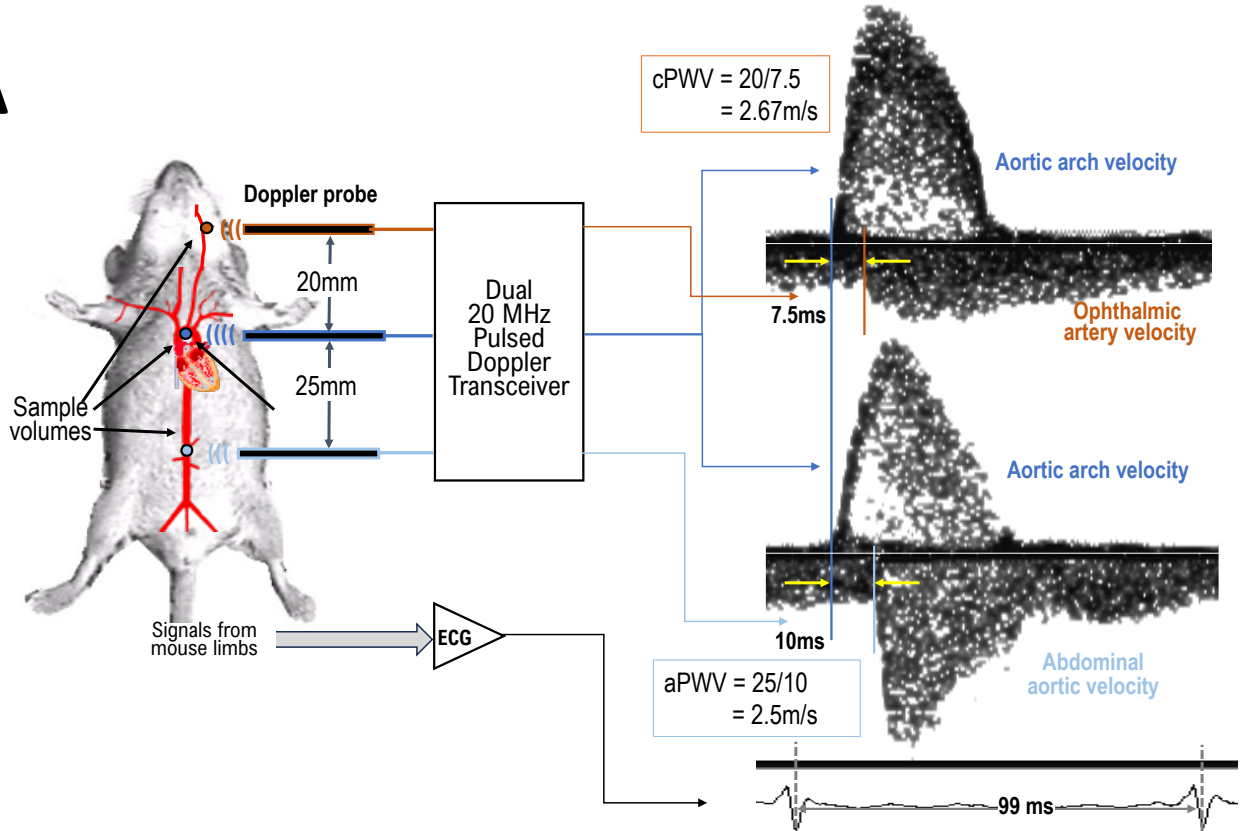
619

620

621

Figure 1

**A**



**B**

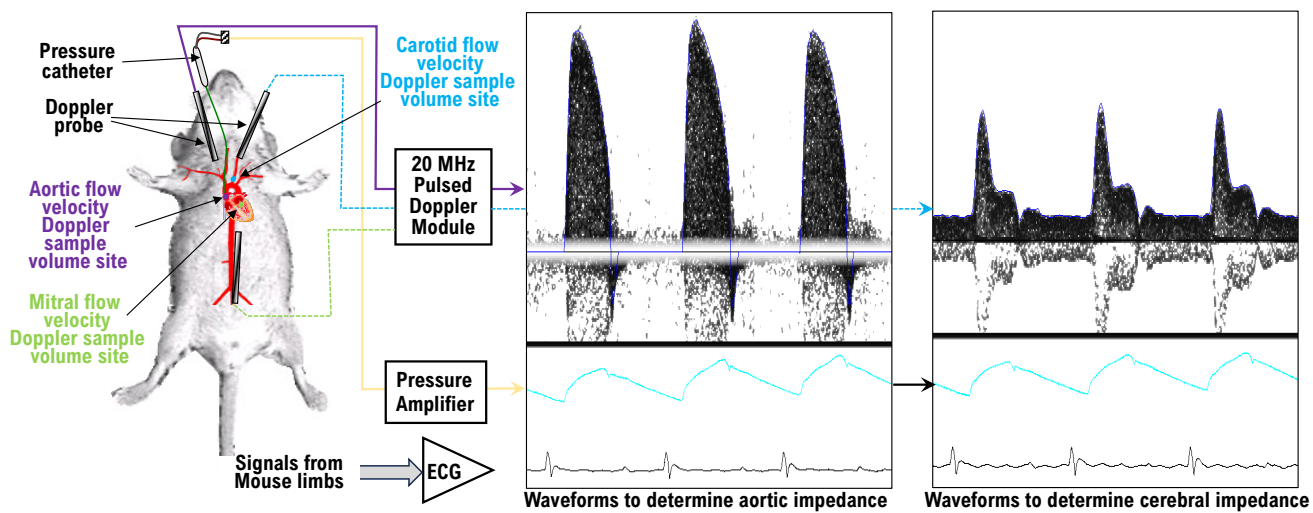
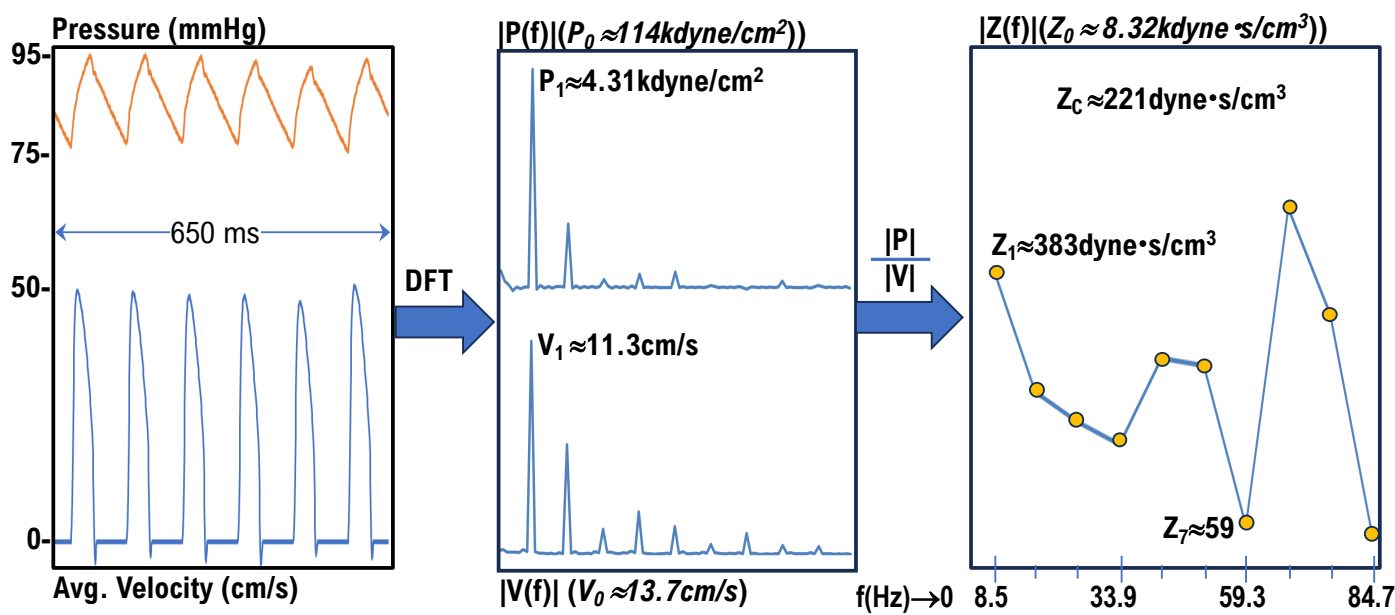
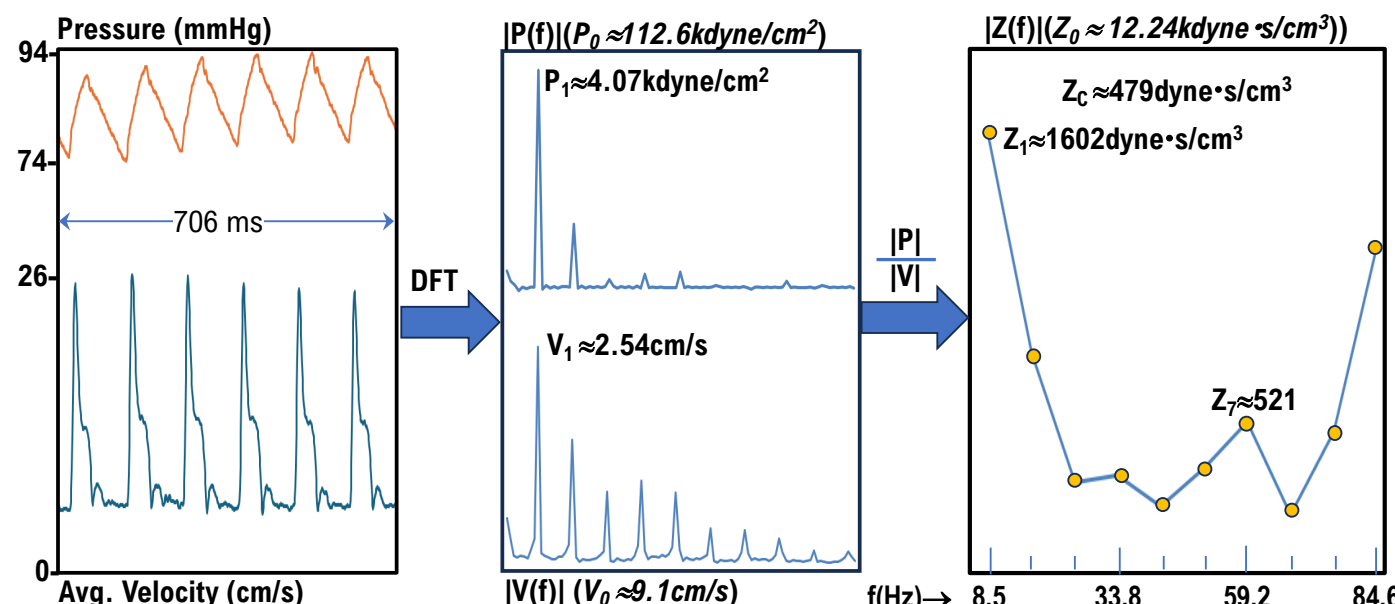
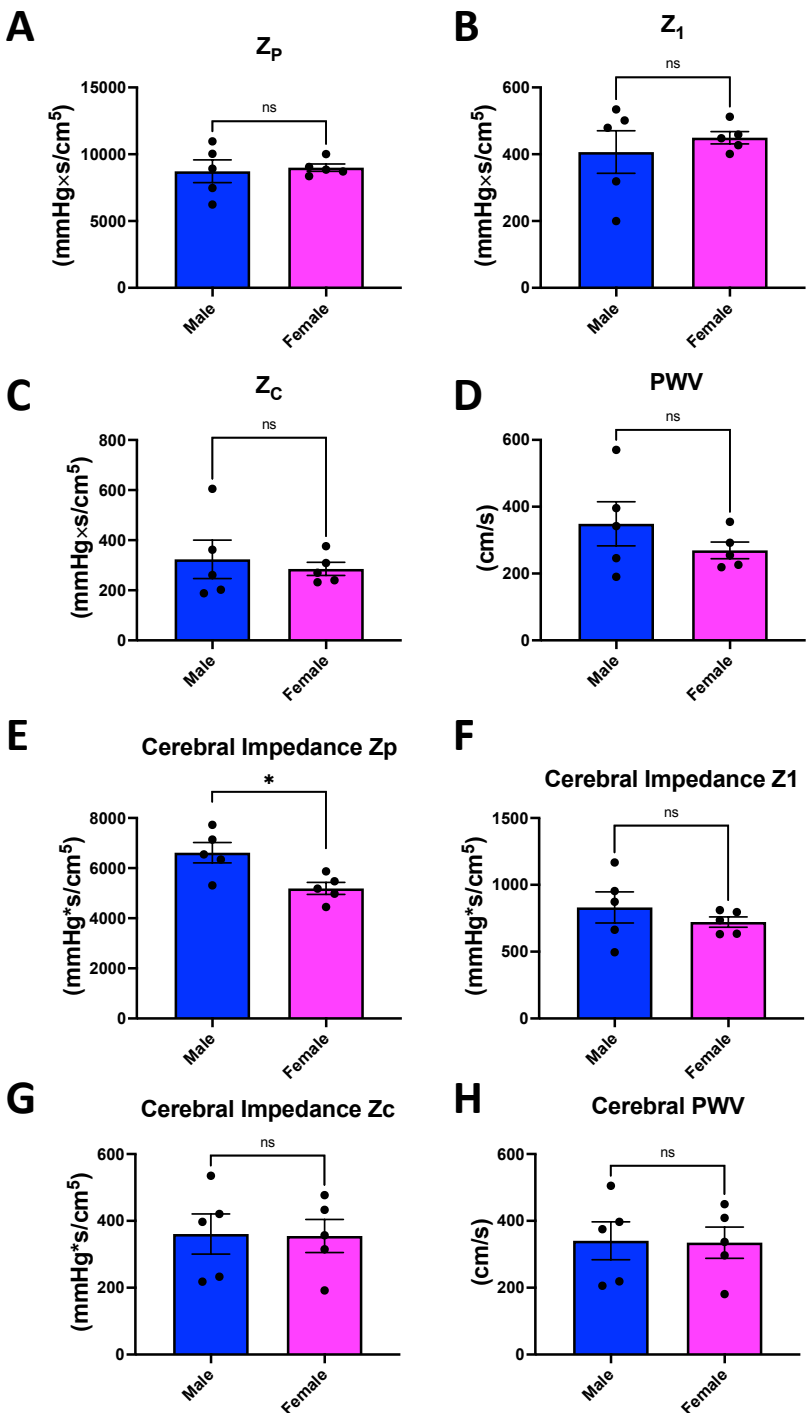
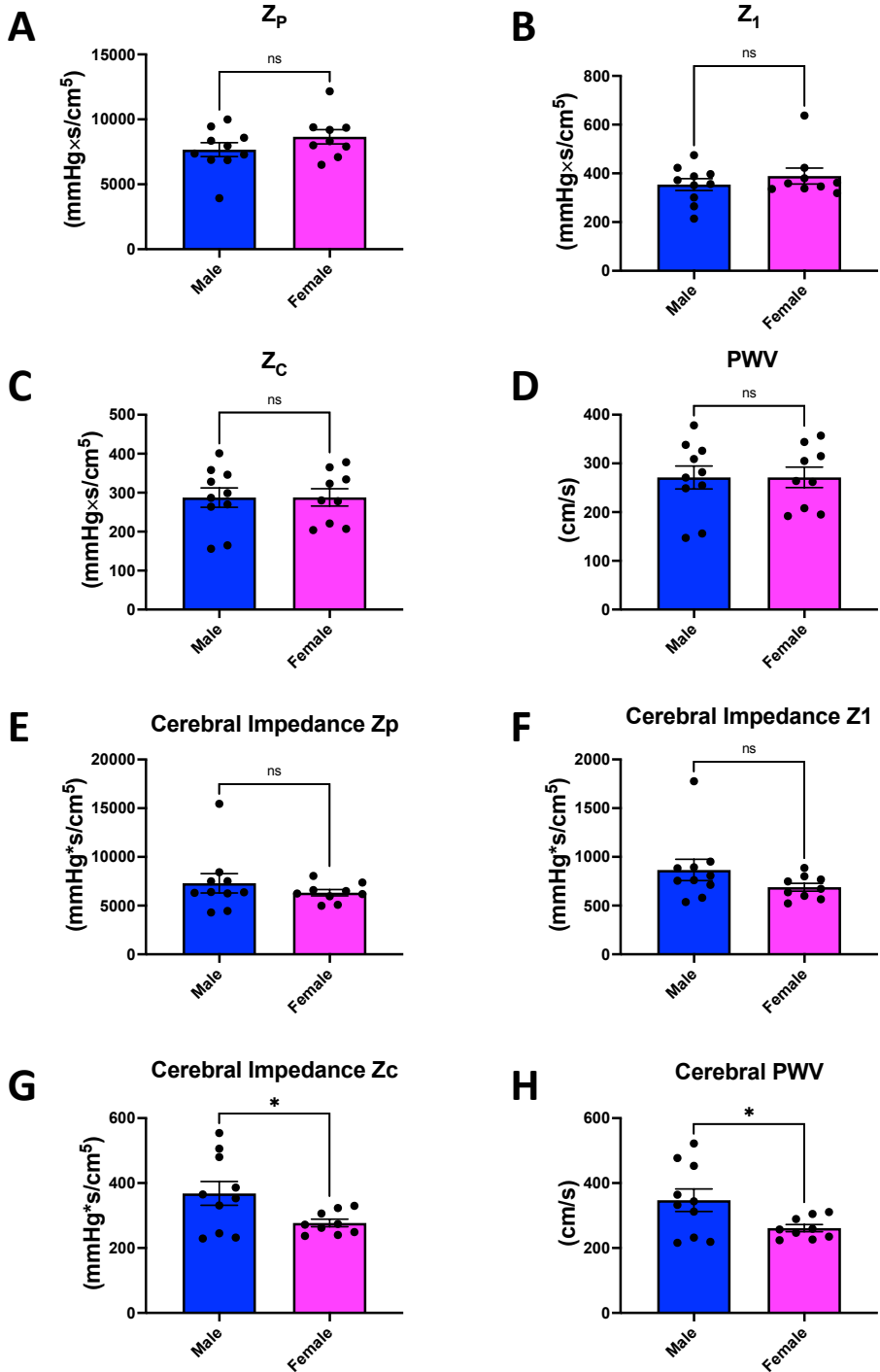


Figure 2

**A****Time Domain****Frequency Domain****Aortic Impedance****B****Time Domain****Frequency Domain****Cerebral Impedance**

**Figure 3**

**Figure 4**

# Figure 5

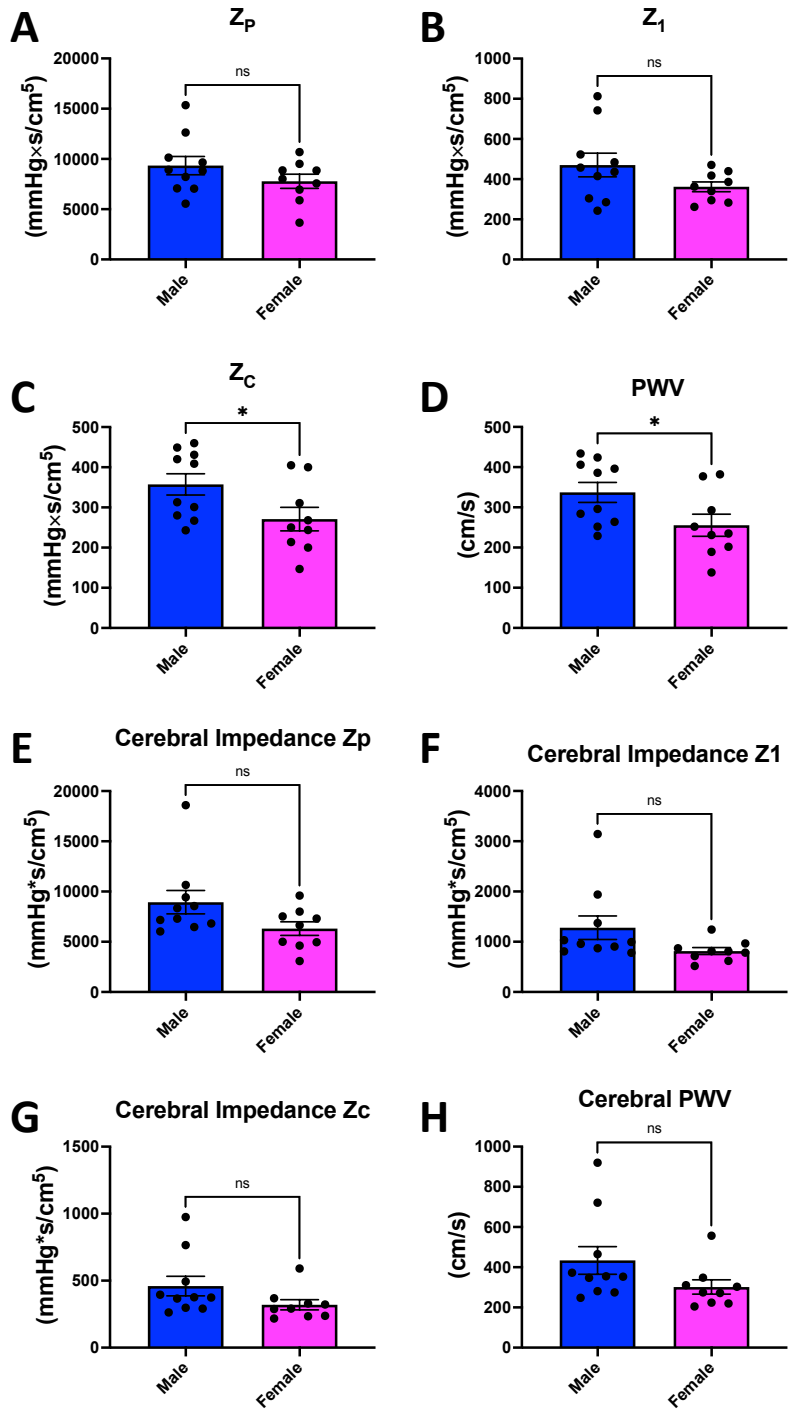
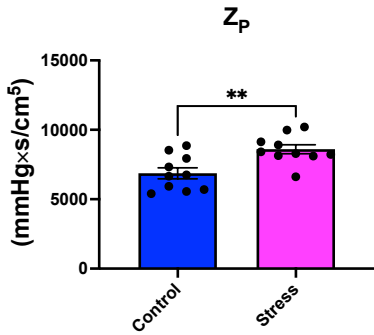
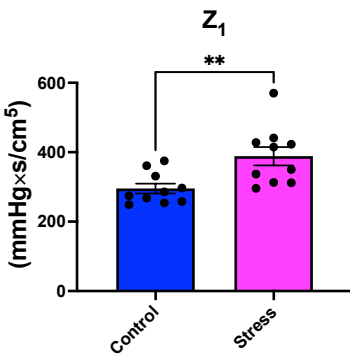


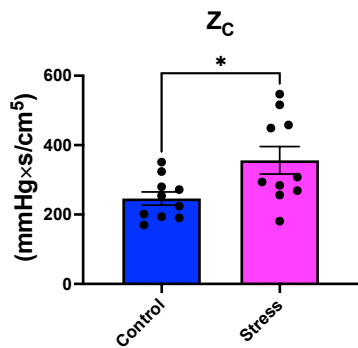
Figure 6 A



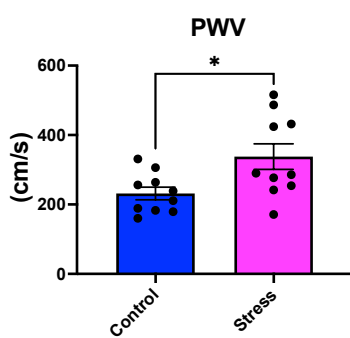
B



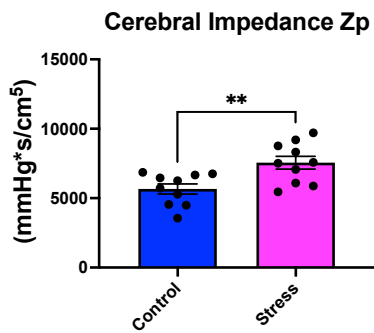
C



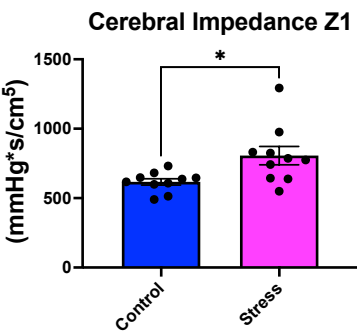
D



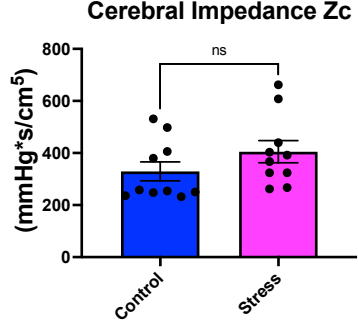
E



F



G



H

